Asian Research Journal of Mathematics

Volume 19, Issue 4, Page 15-30, 2023; Article no.ARJOM.96739
ISSN: 2456-477X

Laminar Plumes from a Line Source and Their Possible Flow Behaviours

Alabodite Meipre George [a*], Evans Fiebibiseighe Osaisai [a] and Nicholas Dienagha [a]

[a] *Department of Maths/Computer Science, Niger Delta University, Wilberforce Island, Bayelsa State, Nigeria.*

Authors' contributions

This work was carried out in collaboration among all authors. All authors read and approved the final manuscript.

Article Information

DOI: 10.9734/ARJOM/2023/v19i4650

Open Peer Review History:
This journal follows the Advanced Open Peer Review policy. Identity of the Reviewers, Editor(s) and additional Reviewers, peer review comments, different versions of the manuscript, comments of the editors, etc are available here: https://www.sdiarticle5.com/review-history/96739

Original Research Article

Received: 03/01/2023
Accepted: 18/02/2023
Published: 06/03/2023

Abstract

Numerical investigation on laminar plumes that under goes buoyancy reversal had just been made, fixing both Re & Pr and varying Fr during the simulations. Water density was taken as a quadratic function of temperature. The result showed some side-to-side flapping and bobbing motion after the core of the fountain were exposed together with head detachment behaviour. At the fountains core, profiles of vertical velocity component show that decrease in vertical velocity with height is not smoother even at higher Froude numbers as compared to the case in our previous study for ($Re = 50$). Empirically determined scalings laws for fountain height and time to attain maximum height were obtained. Initially rising plumes were symmetric and takes much longer time to attain a fully developed stage as Fr increases before sufficient dense fluid is produced to halt their rise. Generally, we can conclude that with the quadratic dependence relation assumption, Irrespective of the flow parameters used within the Reynolds number range $50 \leq Re \leq 100$ and

*Corresponding author: E-mail: alaboditemgeorge@ndu.edu.ng, georgianalgebra@gmail.com;

Prandtl number $Pr = 7 \,\&\, 11.4$ the flow behaviour remains the same. Except for the behaviour in the profiles of vertical velocity that show some slight differences as compared to our earlier investigation, and the Froude number that represents the balance between inertia and buoyancy forces (responsible for the variation in the fountains heights).

Keywords: Cold water; line plume; buoyancy reversal; numerical simulation.

1 Introduction

Buoyancy driven flows are of great interest based on the likelihood of buoyancy reversal especially in rising plumes in cold fresh water; which may be due to the nonlinear relation between temperature and density in water. If we introduce a warm water discharge at the floor of a lake or somewhere close to it, where the ambient dense fluid is considered to be quiescent with its temperature below the temperature of maximum density (approximately $4^{\circ}C$) in fresh water. Mixing is bound to occur between the two fluid (warm water and ambient cold water) which will in turn produce water that is denser than both the warm discharge and the ambient fluid, a process called cabbeling by Foster [1] as we have also recorded in [2]. In this, it is expected that a plume of warm water which at first rises due to its greater buoyancy may under go buoyancy reversal and form a fountain as the most dense mixed fluid descend to the lake bed: see Fig. 1. Furthermore, if the medium into consideration dose not have greater depth, then the most buoyant fluid could rise to the lake surface and spread outwards forming surface gravity current. But then, further entrainment of cold water into the gravity current will then lead to buoyancy reversal as a result of cabbeling, and the gravity current will halt even as the most dense fluid descend to the lake bed forming a fountain: see Fig. 2. Details of such flow scenarios can also be found in [3] so as to gain more insight.

Power station cooling water discharges are practical examples of such scenarios where flows of this nature can be found. This cooling water is usually discharged at a temperature approximately $10^{\circ}C$ above that of the ambient water [3, 4, 5]. This implies that the warm discharge will definitely be less dense than that of the ambient fluid and as a result of that, the less dense fluid will initially form a rising plume. But then, if the surrounding fluid is below the temperature of maximum density, buoyancy reversal due to cabbeling will occur [3]. At that point, mixed fluid close to the temperature of maximum density will then descend to the floor. In a particular investigation, Hoglund and Spigarelli [6] were able to observe water at a temperature of $5.7^{\circ}C$ at the bed of lake Michigan in the vicinity of a power station outfall while the natural ambient temperature was $0.5^{\circ}C$, and concluded that the relatively warm but dense water had been formed by this means. Meanwhile, it is supposed that power station warm discharges will obviously be fully turbulent: but then, laboratory experiments by Bukreev and Gusev [7] could produce plumes with much lower Reynolds numbers, meaning that such flows may be laminar or in transition to turbulence. However, previous authors have also investigated on both laminar and turbulent fountains using the normal linear dependence relation assumption of density on temperature, where a negatively buoyant fluid is being injected upwards into a less dense ambient [3]. We can consider the following [3, 8, 9, 10] for a more detailed literature to avoid repetition.

These authors [11] in their work have also shown that the fountains were symmetric and steady up to $Fr \approx 2.25$. But as Froude numbers increases, lateral oscillations (a flapping motion) were found and these were periodic for $Fr \leq 4$ but chaotic for $Fr > 4$. Scaling laws for their fountain's height was found to be $Z_m/x_0 \sim Fr^{1.15}$ in the periodic oscillation regime, and $Z_m/x_0 \sim Fr^{4/3}$ for the chaotic flapping regime. Though, with a parabolic source velocity profile [12] obtained different values for the transition Froude numbers, and a Fr^2 scaling for fountain height in the periodic flapping regime as also recorded in [3]. Experimental investigations by [13, 14 & 15] have also also shown different possible fountain behaviours, and that transitions between the possible behaviours are also dependent on both Froude and Reynolds numbers. However, it is also clear that the above reviewed cases have all considered flows where the buoyancy flux opposes the momentum flux at the source. Meanwhile, less attention had just been given to fountains that resulted arising buoyancy reversal as also recorded in [3]. Note

that buoyancy reversal requires a nonlinear relation between density and the mixing ratio of the warm discharge and the ambient fluids. If we assume density to be a quadratic function of mixing ratio, with the mixed fluid that is less dense than the mean of the constituents densities [3] These authors [16] have also used the entrainment assumption of Morton, Taylor and Turner [17] by injecting upwards a dense fluid into an ambient of less dense fluid. This we can compare to a case where warm water is injected downwards into an ambient that is colder than the T_m, where the plume may form an inverted fountain or continue to sink without being arrested as also recorded in [3].

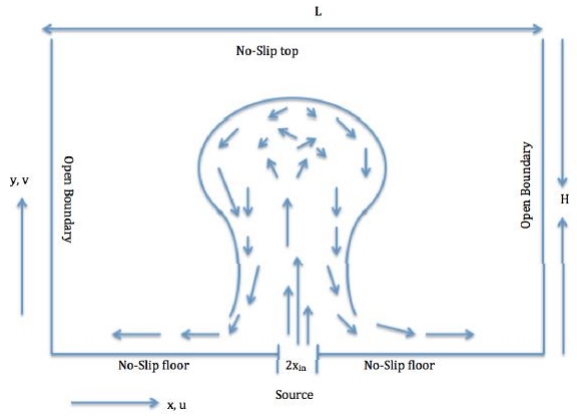

Fig. 1. Schematic of plume with buoyancy reversal, also showing domain for computations

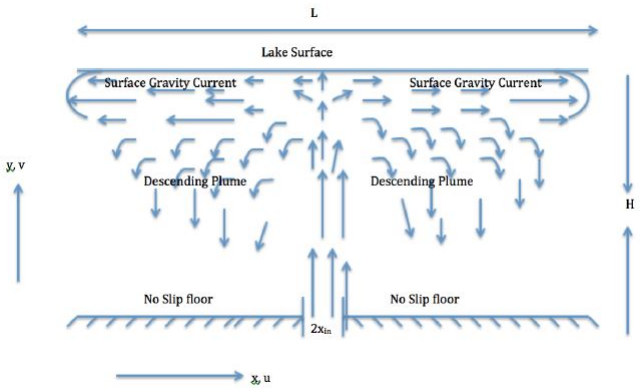

Fig. 2. Schematic of plume reaching lake surface before experiencing buoyancy reversal

Kay [18] in his work have also studied the case where warm water was injected upwards into a cold ambient, and uses the classical entrainment assumption. The difficulty here is that it can model a plume up to the level where it is arrested, but cannot really justify that of the reversed flow in a fountain [3]. The experimental study by Bukreev and Gusev [7] involved the injection of warm water upwards into an ambient below the temperature of maximum density at low Reynolds number, so that a laminar fountain was produced; as in the turbulent case studied by Turner [19]. Both authors noted a periodic oscillations of the fountain height, and that as time progresses, the descending dense water would be displaced to one side of the rising plume. But then, they only

gave few examples without any systematic investigation of how the flow depends on source conditions [3].

It is worth noting that we have also considered laminar fountains with the assumption that density was taken as a quadratic function of temperature numerically. At the source, the discharge has a parabolic velocity profile, with fixed $Re = 50$, $Pr = 7$ and varied Froude number over the range $0.2 \leq Fr \leq 2.5$. Our results showed some similarities to those fountain resulting from the injection of a negatively buoyant fluid upward into a less dense ambient. The plumes are initially symmetric and later under goes head detachment behaviour as they approaches their maximum height. (see [3] for more details). However, our empirically determined data could only allow us to identify a single regime of Froude number dependence of fountains height. But then, these authors [11] were able to identified three regimes of Froude number dependence for the fountain's height which reflects the different behaviours (e.g. between steady and unsteady flow). Meanwhile, we have not been able to observe such differences in in the regime of flow, which have really triggered the present investigation.

Thus, the aim of this paper is to further carryout a computational investigation with this assumption to know whether there is a different regime for $Fr > 2$. we adopt all the assumption as recorded in [3] except for Reynolds and Prandtl numbers that we have kept fixed through out the simulations, $Re = 100$ and $Pr = 11.4$, and vary the Froude number $0.2 \leq Fr \leq 5$ which represents the balance between inertia and buoyancy forces. The choice of $Pr = 11.4$ is more appropriate especially for the power station warm discharge in cold fresh water, where mixing will certainly produce mixture at T_m. Computational domain length and height will be kept constant, where length $L = 70x_{in}$, i.e., $0 \leq X \leq 70$, and a domain height $H = 56x_{in}$ i.e., $0 \leq Y \leq 56$.

2 Model Formulation and Governing Equations

The behaviour of laminar plumes that form fountains due to buoyancy reversal is being considered. This is very important and possible because of the nonlinear relation between density ρ and temperature T. Thus, the relation below is useful for this study,

$$\rho = \rho_m - \beta(T - T_m)^2 \tag{1}$$

This we think gives an appropriate fit to the experimentally determined density of fresh water at temperature below $10^{\circ}C$ if we consider $T_m = 3.98^{\circ}C$, $\rho_m = 1.000 \times 10^3\ kg.m^{-3}$ and $\beta = 8.0 \times 10^{-3}\ kg.m^{-3}(^{\circ}C)^{-2}$ [3, 20, 21] and all other fluid properties (e.g. viscosity, thermal diffusivity) are assumed constant. We also assume that the flow is time dependent and two dimensional, and that the liquid property is constant except for the water density, which changes with temperature and in turn results to the buoyancy force. The source velocity profile is assumed parabolic as for laminar Poiseuille flow (cf. [11]),

$$v(x, 0) = \frac{3}{2} v_{in}[1 - (\frac{x}{x_{in}})^2] \tag{2}$$

The input fluid temperature is T_{in} is assume constant at the centre of the domain and a uniform initial ambient temperature T_∞. Dimensions for the domain of computation are not suitable length scales, as we consider them reliable for conditions at the sides and top to have no effect on the plume. Thus, we non-dimensionalise the coordinates x, y, velocity components u, v, time t, pressure p and temperature T by

$$U = \frac{u}{v_{in}} \quad V = \frac{v}{v_{in}} \quad X = \frac{x}{x_{in}} \quad Y = \frac{y}{x_{in}} \quad \tau = \frac{t}{x_{in}/v_{in}} \quad P = \frac{p}{\rho v_{in}^2} \quad \phi = \frac{T - T_\infty}{T_m - T_\infty}, \tag{3}$$

where x and u are horizontal, y and v are vertical [2].

We can also define our dimensionless parameters, the Reynolds Re, Prandtl Pr and Froude Fr numbers, by

$$Re = \frac{v_{in}x_{in}}{\nu}, \quad Pr = \frac{\nu}{\alpha}, \quad Fr^2 = \frac{\rho_m v_{in}^2}{g\beta(T_m - T_\infty)^2 x_{in}}, \tag{4}$$

where ν and α are the respective diffusivities of momentum and heat, $\nu = \mu/\rho$ and $\alpha = k/\rho c_p$. Where, μ is viscosity, k is thermal conductivity and c_p is specific heat capacity. In terms of these dimensionless variables and parameters, the continuity equation, the horizontal and vertical momentum equations and the thermal energy equation are given as:

$$\frac{\partial U}{\partial X} + \frac{\partial V}{\partial Y} = 0 \tag{5}$$

$$\frac{\partial U}{\partial \tau} + U\frac{\partial U}{\partial X} + V\frac{\partial U}{\partial Y} = -\frac{\partial P}{\partial X} + \frac{1}{Re}(\frac{\partial^2 U}{\partial X^2} + \frac{\partial^2 U}{\partial Y^2}) \tag{6}$$

$$\frac{\partial V}{\partial \tau} + U\frac{\partial V}{\partial X} + V\frac{\partial V}{\partial Y} = -\frac{\partial P}{\partial Y} + \frac{1}{Re}(\frac{\partial^2 V}{\partial X^2} + \frac{\partial^2 V}{\partial Y^2}) + \frac{1}{Fr^2}[\phi^2 - 2\phi] \tag{7}$$

$$\frac{\partial \phi}{\partial \tau} + U\frac{\partial \phi}{\partial X} + V\frac{\partial \phi}{\partial Y} = \frac{1}{RePr}(\frac{\partial^2 \phi}{\partial X^2} + \frac{\partial^2 \phi}{\partial Y^2}) \tag{8}$$

Our initial conditions are an undisturbed, homogeneous medium as also given in [2].

$$U = 0, \quad V = 0, \quad \phi = 0, \quad for \quad \tau < 0 \tag{9}$$

For $\tau \geq 0$ we have boundary conditions as follows. On the side walls:

$$\frac{\partial U}{\partial X} = 0, \quad \frac{\partial V}{\partial X} = 0, \quad \frac{\partial \phi}{\partial X} = 0 \quad at\ X = \pm\frac{L}{2x_{in}} \tag{10}$$

At the plume source:

$$U = 0, \quad V(X,0) = 1.5(1 - X^2), \quad \phi = \phi_{in} \quad for\, |X| \leq 1 \quad at\, Y = 0 \tag{11}$$

Elsewhere on the floor of the domain:

$$U = 0, \quad V = 0, \quad \frac{\partial \phi}{\partial Y} = 0, \, for \quad |X| > 1 \quad at\, Y = 0 \tag{12}$$

At the top of the domain:

$$U = 0, \quad V = 0, \quad \frac{\partial \phi}{\partial Y} = 0\, at\, Y = \frac{H}{x_{in}} \tag{13}$$

Reynolds number $Re = 100$ and Prandtl number $Pr = 11.4$ will be fixed throughout this investigation varying Froude number $0.2 \leq Fr \leq 5$. The dimensionless temperature $\phi_{in} = 2.5$ at the centre, and this is equivalent to a warm discharge at $10^\circ C$ into an ambient temperature at $0^\circ C$. Numerical solution of the above equations is by the means of COMSOL Multiphysics software. This is a commercial package that uses finite element solver with discretization by the Galerkin method and stabilisation to prevent spurious oscillations. We have used the "Extremely fine" setting for the mesh. Time stepping is by COMSOL's Backward Differentiation Formulas [3]. Further information about the numerical methods is available from the COMSOL Multiphysics website [22]. Results will be illustrated mainly by surface temperature plots of dimensionless temperature on a colour scale from dark red for the ambient temperature $\phi = 0.0$, through yellow to white for the source temperature $\phi = 2.5$. Note that $\phi = 1.0$ corresponds to the temperature of maximum density. Meanwhile, $\phi = 2$ correspond to the temperature at which warm water has the same density as that of the ambient cold water [3].

3 Results

The following Figs. $3, 4, 5, 6, 7, 8$ *and* 9, show the evolution of plumes with different Froude numbers $Fr = 1, 3, 4$ *and* 5; in panels (a), (b), (c), (d) respectively for the various Froude numbers. After the release of warm discharge at the source, fluid in the plume with the greatest buoyancy ($Fr = 1$) is becoming dense and approaching its maximum height within the time frame $\tau = 5$ (see Fig. 3a) as compared to those in the other panels. At this point, cabbeling had begun even though significant amount of dense fluid had not been noticed on the floor. As time progresses, it is obvious that plumes with the greatest buoyancy have attained their maximum height and collapsed. This indicates that plumes with higher source Froude numbers rise more slowly, but later attain greater maximum heights. Though, all the plumes will definitely stop rising, having begun to lose momentum as a result of cabbeling [3]. Fig. (4a & 5a) shows that at $\tau = 20$ & 40 a significant amount of dense fluid has already been shed from the outside of the plume with $Fr = 1$ and spreading outwards on the floor. However, plumes with higher Froude numbers have less vigorous mixing and as such they appear symmetric up to $\tau = 20$ which account for their maximum rise heights (see Fig. 3 & 4). As time further progresses, all the plumes lose their symmetric shape through a process of head detachment (Figs. 5b,& c; 6c & d; 7c & d; 8d). This was as a result of the fact that the head of the plume had become denser than the neck beneath it and in turn resulted in the process of head detachment. After then, there was an interaction between the sinking detached head and the faster rising fluid in the neck which in turn also causes the head to be deflected from one side to the other [3].

Having that the supply of warm fluid from the source is continuous and that of the production of dense fluid; this resulted to a continuous flapping and bobbing motion of the plume (i.e., deflection of the detaching heads resulted to a side-to-side flapping, which in turn exposes the plume's core after which led to a vertical bobbing motion) [3]. The behaviours as presented are very similar to our previous work [3], where we have considered Reynolds and Prandtl numbers fixed through out the simulations, $Re = 50$ and $Pr = 7$, and vary the Froude number $0.2 \leq Fr \leq 2.5$ so as to carryout a comparative analysis with those by Srinarayana et al. [11]. In that investigation, we were able to record approximately all the behaviours as we have observed here despite the fact that there is a variationin the flow parameters. However, both flapping and bobbing motion has also been recorded by Vinoth and Panigrahi [23] in non-Boussinesq laminar fountains at higher Froude numbers. Results by Srinarayana et al. [11] for a laminar plane fountain with $Fr = 8$ and a linear dependence of density on temperature have also shown some similarities with our case here, especially in the case of the flapping from side to side behaviour. For that of the vertical bobbing behaviour, Turner [19] in a turbulent plume with reversing buoyancy have also recorded that [3]. Whereas, the dense fluid on the floor spread outwards horizontally as density current (see Fig. 4a, 5a, 6a, 7a, 8a & b, 9a & b). This part also appears similar to those by George & Osaisai [24, 25, 26]. Though, the motion in the gravity current in this present investigation is slow, which may be due to the small density difference between the current and the ambient. The spread of the current is steady except when it is perturbed by the arrival of new dense fluid from a detached head, which may cause oscillations downstream: unlike [24 - 26] where the perturbation is as a result of the development of kelvin-Helmholtz instabilities at the interaction layer between the current and the ambient fluid.

Profiles of temperature and the various velocity components up the centre-line of the plume (X = 0) have also been considered in Figs. $10, 11$ & 12 which will enable us to gain more insight in such flows. Fig. 10 show the profiles of temperature for the four Froude number cases at five different levels. These profiles agree to the fact that plumes with higher Froude number could penetrate the ambient fluid farther to attain a greater height. Whereas, there was vigorous mixing leading to a reduced penetration height for plumes with smaller Froude numbers. Though, heights of the various plumes decreases after maximum penetration. Furthermore, the results also show a region where temperature appears uniform at some point immediately above the source; especially for the higher Froude number cases [3]. This indicates that warm water could still be retained even up to that level because of the slow mixing rate and in turn enhances more penetration. From the profiles, it is also clear that decrease in temperature with height is not monotonic. Some of these fluctuations reaches their local maximum before decreasing sharply to the ambient temperature [3].

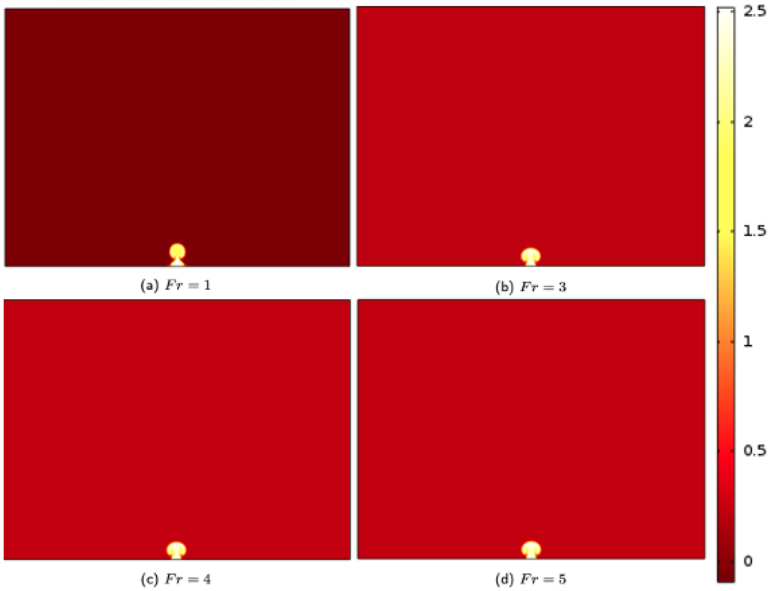

Fig. 3. Temperature field at time $\tau = 5$ for plumes with $Re = 100$, $Pr = 11.4$, $\phi_{\text{in}} = 2.5$ and (a) $Fr = 1$, (b) $Fr = 3$, (c) $Fr = 4$ and (d) $Fr = 5$

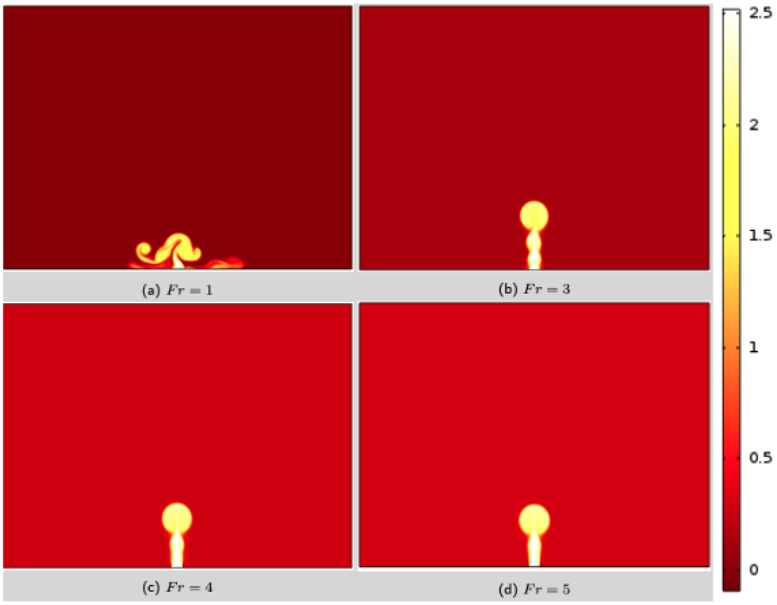

Fig. 4. Temperature field at time $\tau = 20$ for plumes with $Re = 100$, $Pr = 11.4$, $\phi_{\text{in}} = 2.5$ and (a) $Fr = 1$, (b) $Fr = 3$, (c) $Fr = 4$ and (d) $Fr = 5$.

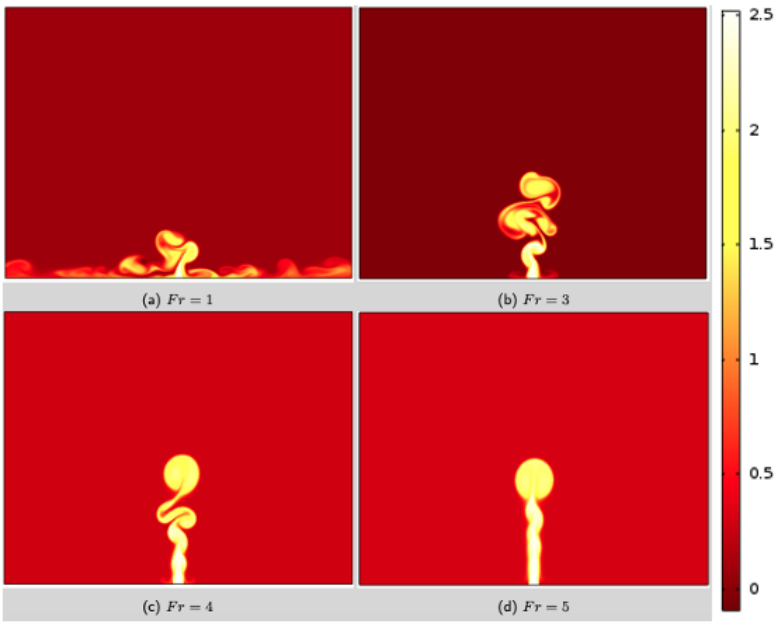

Fig. 5. Temperature field at time $\tau = 40$ for plumes with $Re = 100$, $Pr = 11.4$, $\phi_{\text{in}} = 2.5$ and (a) $Fr = 1$, (b) $Fr = 3$, (c) $Fr = 4$ and (d) $Fr = 5$

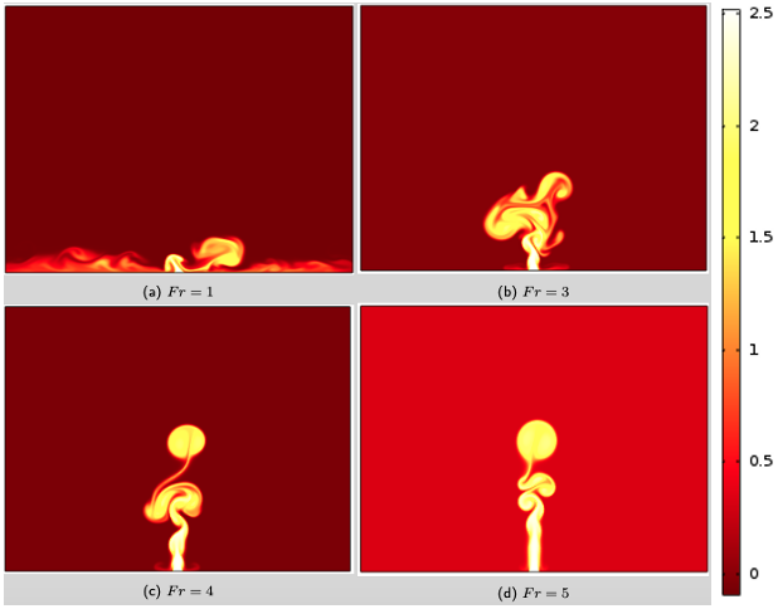

Fig. 6. Temperature field at time $\tau = 50$ for plumes with $Re = 100$, $Pr = 11.4$, $\phi_{\text{in}} = 2.5$ and (a) $Fr = 1$, (b) $Fr = 3$, (c) $Fr = 4$ and (d) $Fr = 5$.

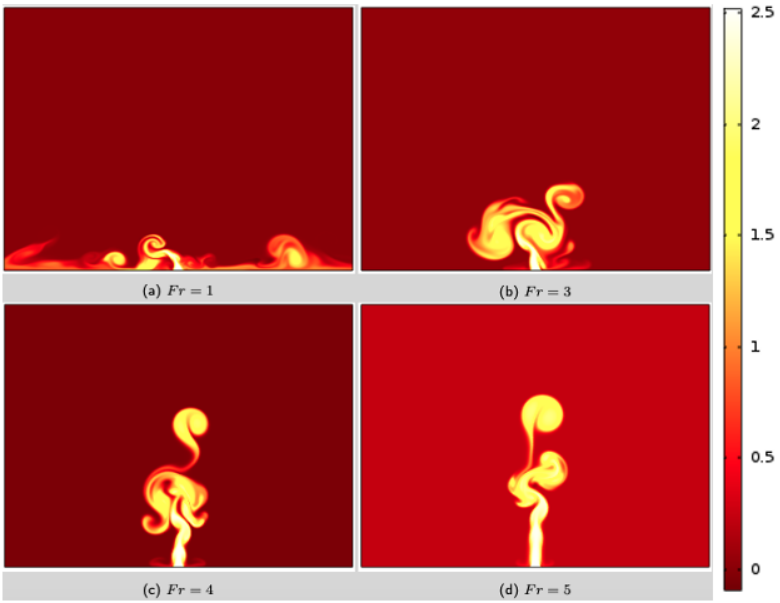

Fig. 7. Temperature field at time $\tau = 60$ for plumes with $Re = 100$, $Pr = 11.4$, $\phi_{\text{in}} = 2.5$ and (a) $Fr = 1$, (b) $Fr = 3$, (c) $Fr = 4$ and (d) $Fr = 5$.

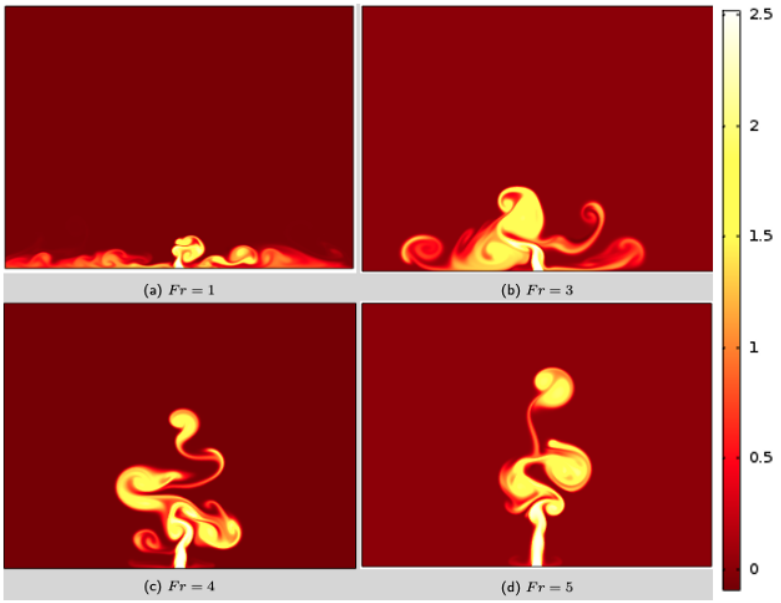

Fig. 8. Temperature field at time $\tau = 80$ for plumes with $Re = 100$, $Pr = 11.4$, $\phi_{\text{in}} = 2.5$ and (a) $Fr = 1$, (b) $Fr = 3$, (c) $Fr = 4$ and (d) $Fr = 5$.

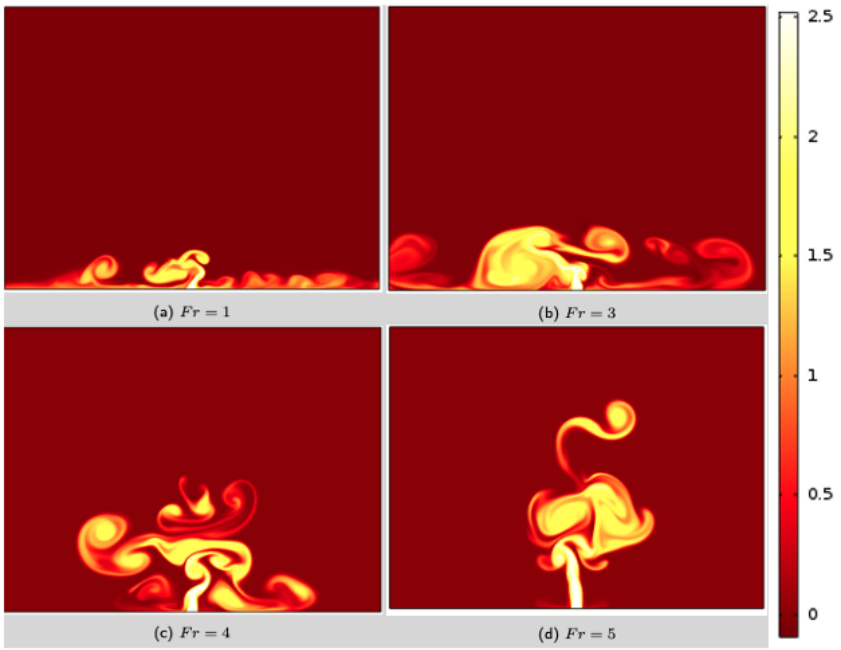

Fig. 9. Temperature field at time $\tau = 100$ for plumes with $Re = 100$, $Pr = 11.4$, $\phi_{\text{in}} = 2.5$ and (a) $Fr = 1$, (b) $Fr = 3$, (c) $Fr = 4$ and (d) $Fr = 5$

Table 1. Maximum plume height Z_n and time taken to reach that height at Froude numbers $0.2 \leq Fr \leq 5$

Fr	τ_n	Z_n	Fr	τ_n	Z_n	Fr	τ_n	Z_n
0.2	1.8	2.55	2.5	27.6	18.978	4.8	73.5	40.314
0.5	4.6	4.8	2.8	33.6	21.504	5.0	75.6	42.524
0.8	7.8	6.938	3.0	36.0	22.59			
1.0	10.0	8.051	3.2	41.0	24.697			
1.2	12.6	9.905	3.5	47.0	27.512			
1.5	16.6	12.706	3.8	52.0	31.025			
1.8	19.6	14.77	4.0	56.6	33.241			
2.0	22.6	16.233	4.2	63.0	34.681			
2.2	24.6	17.46	4.5	67	37.987			

Profiles of vertical velocity component are shown in Fig. 11; which indicates some sort of intense fluctuations ranging from the source with some degree of downward velocities within some time interval. Where the downward velocities indicates descending fluid and this behaviour is common to all the Froude number cases considered. There is a significant difference in the profiles of vertical velocity component as compared to those by [3]. Those results showed that fluctuations in the vertical velocities decreases (appears smother) with increase in Froude numbers. Though, the results records some level of downward velocities within the top most part of the plume after it has reached its maximum height and start to sink. Whereas, results in this present investigation showed that even at higher Froude numbers the decrease in vertical velocity with height is not smoother and this might be as a result of the slight increase in Reynolds number that might have enhanced slightly intense mixing as

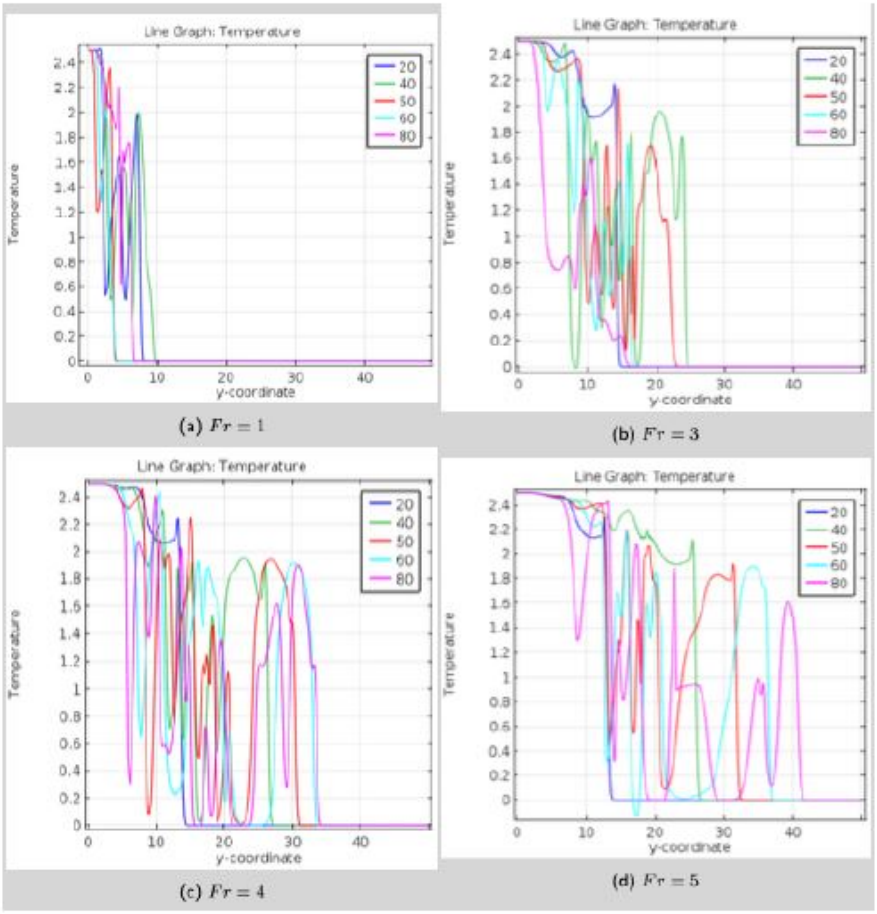

Fig. 10. Dimensionless centreline temperature distribution $\phi(0, y)$ at times $\tau = 20, 40, 50, 60, 80$, for plumes with $Re = 100$, $Pr = 11.4$, $\phi_{\text{in}} = 2.5$ and (a) $Fr = 1$, (b) $Fr = 3$, (c) $Fr = 4$ and (d) $Fr = 5$

compared to the former. Profiles of horizontal velocity component up the plume centre-line are also shown in Fig. 12. These profiles show that there is a strong side-to-side flapping motion close to the source within the time range considered. Though, as Froude numbers increases this side-to-side flapping motion takes little longer time to develop and is less intense but penetrate to a greater heights.

We have considered the maximum rise height Z_n attained by the plume and the time τ_n taken to attain that height and tabulated for a range of Froude numbers as shown in Table 1, and plotted in Figs. 13 and 14. The results as recorded here also appears very similar to those by George & Kay [3] where, they could only identify a single regime of Fr-dependence which is similar to what we have also recorded here. This we have shown by the straight lines in Figs. 13 and 14, representing the best fit power laws obtained by linear regression of $\log Z_n$ and $\log \tau_n$ on $\log Fr$ from our empirically determined data set: where R^2 is the regression coefficient in each case.

$$Z_n = 8.9394 Fr^{0.9063} \qquad [R^2 = 0.9888] \tag{14}$$

$$\tau_n = 10.461 Fr^{1.1841} \qquad [R^2 = 0.9953], \tag{15}$$

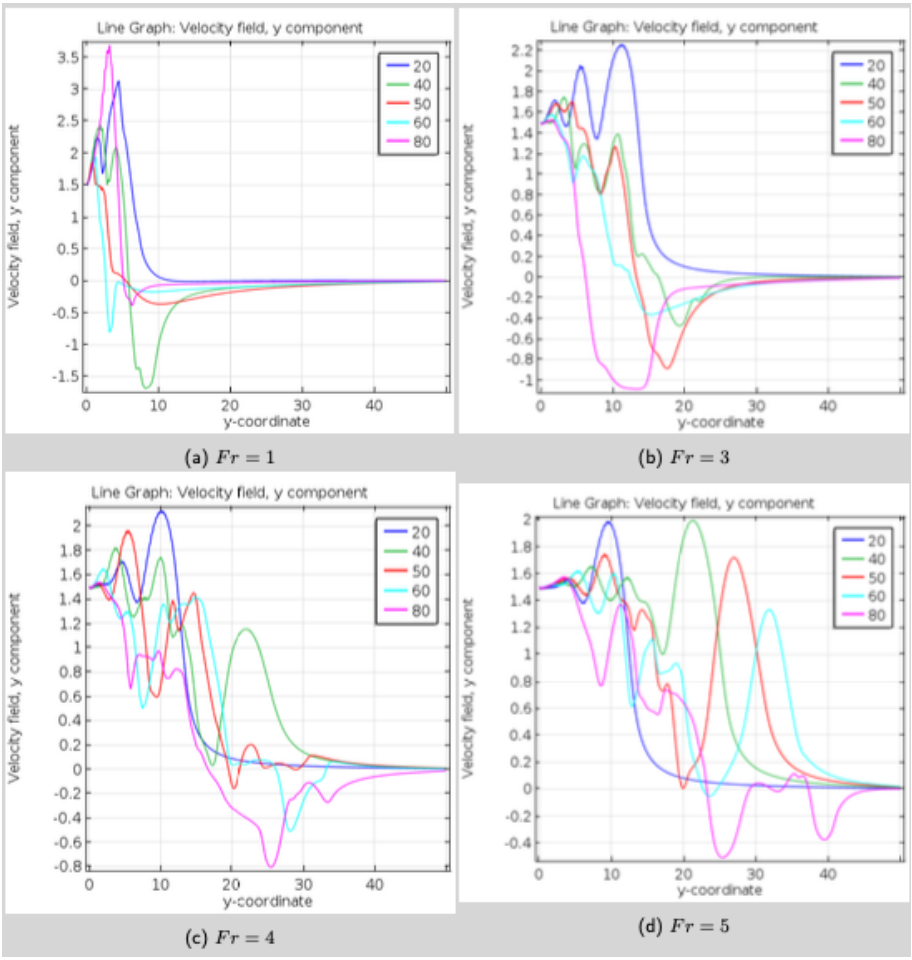

Fig. 11. Dimensionless centreline Y-component velocity distribution $V(0, y)$ at times $\tau = 20, 40, 50, 60, 80$, for plumes with $Re = 100$, $Pr = 11.4$, $\phi_{\text{in}} = 2.5$ and (a) $Fr = 1$, (b) $Fr = 3$, (c) $Fr = 4$ and (d) $Fr = 5$

As regards the main focus of this present study, the Froude number range as considered has not guaranteed a different regime of flow. But then, Srinarayana et al. [11] in their work could identify three regimes of flow. Though, they have assumed a linear dependence of density on temperature. One of the unique behaviours with the quadratic dependence assumption is head detachment. In some cases with higher Froude numbers, this detached head could penetrate farther. Having observed this, we are suggesting that much smaller values of Reynolds number and a moderate value of Froude number be reconsidered to know if these behaviours are entirely depended on flow parameters for the laminar flow scenario. Above all, we can conclude that with the quadratic dependence relation assumption, Irrespective of the flow parameters used within the Reynolds number range $50 \leq Re \leq 100$ and Prandtl number $Pr = 7 \,\&\, 11.4$ the flow behaviour remains the same. Except for the behaviour in the profiles of vertical velocity that show some slight differences as compared to our earlier investigation, and the Froude number that represents the balance between inertia and buoyancy forces (responsible for the variation in the fountains heights).

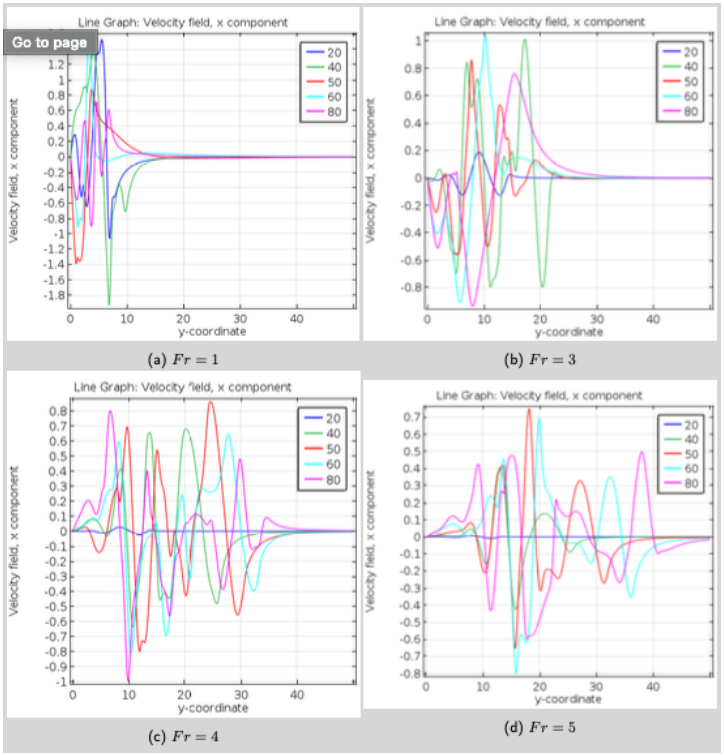

Fig. 12. Dimensionless centreline X-component velocity distribution $U(0, y)$ at times $\tau = 20, 40, 50, 60, 80$, for plumes with $Re = 100$, $Pr = 11.4$, $\phi_{\text{in}} = 2.5$ and (a) $Fr = 1$, (b) $Fr = 3$, (c) $Fr = 4$ and (d) $Fr = 5$

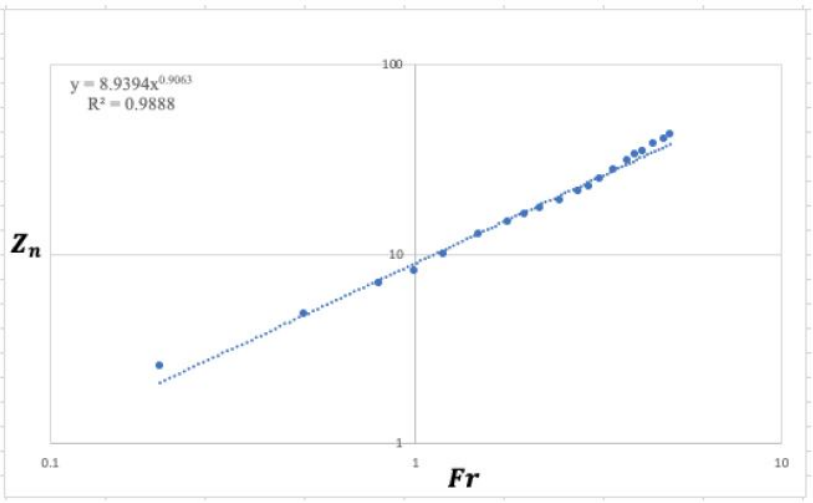

Fig. 13. Variation of maximum plume height with Froude number

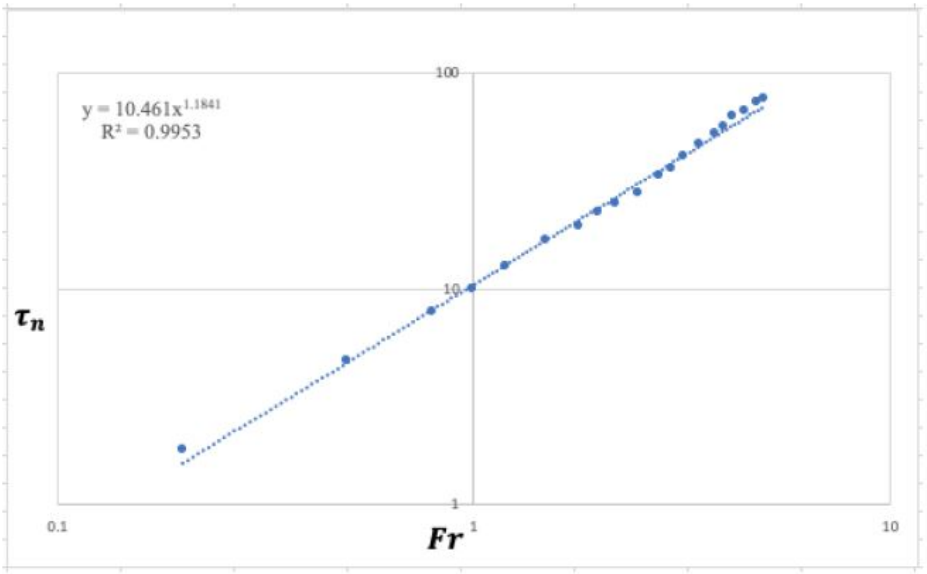

Fig. 14. Time taken for plume to reach maximum height, as a function of Froude number

4 Conclusion

The behaviour of laminar plumes had just been investigated with a quadratic dependence relation assumption by means of a computational model. Time taken to attain a fully developed stage appears longer as compared to our previous studies. As Froude number increases, the plumes with less buoyancy rises more slowly and could attain greater height before sufficient dense fluid is produced to halt their rise because of their slower mixing rate as compared to those with greater buoyancy (smaller Froude numbers). Mixture here require just little mixing to attain buoyancy reversal. Initially, the plumes were symmetric but later display a sideways flapping and vertical bobbing after the core of the fountain were exposed. This seem to be the effect of head detachment after the frontal head had become dense and displaces the plume sideways and sink. At the fountains core, profiles of vertical velocity component show that decrease in vertical velocity with height is not smoother even at higher Froude numbers; which might result from the slight increase in Reynolds number ($Re = 100$) that might have enhanced slightly intense mixing as compared to those of our previous study for ($Re = 50$) [3]. Dense fluid on the floor spread outwards as gravity current. Our empirically determined scalings laws for fountain height and time to attain maximum height (Eqs 14 & 15) are also fairly in line with those by [3] where negative buoyancy is only by means of mixing. They are also to some extent similar to those by [27] for very weak fountains $Z_n \propto Fr^{\frac{2}{3}}$ and $\tau_n \propto Fr^{\frac{4}{3}}$. However, the mechanism for halting the rise of the plumes differ between our case and that of laminar fountains with the linear dependence relation assumption: whereas fountains have negative buoyancy regardless of any mixing. This might be the reason for not justifying a separate regime in our case here. One of the unique behaviours with the quadratic dependence assumption is head detachment. Having observed that with higher Froude numbers, the detached head could penetrate farther, we are suggesting that much smaller values of Reynolds number and a moderate value of Froude number be reconsidered to know if these behaviours are entirely depended on flow parameters for the laminar flow scenario. Furthermore, very higher values of Re be reconsidered for both at transition to turbulence and fully turbulent cases which is most relevant to environmental applications. This we recommend with the aim of determining scalings of plume height against Reynolds number as found by Lin and Armfield [10]. Above all, we can conclude that with the quadratic dependence relation assumption, Irrespective of the flow parameters used within the Reynolds number range $50 \leq Re \leq 100$ and Prandtl number $Pr = 7 \,\&\, 11.4$ the flow behaviour remains the same.

Except for the behaviour in the profiles of vertical velocity that show some slight differences as compared to our earlier investigation, and the Froude number that represents the balance between inertia and buoyancy forces (responsible for the variation in the fountains heights).

Competing Interests

Authors have declared that no competing interests exist.

References

[1] Foster TD. An analysis of the cabbeling instability in sea water. Journal of Physical Oceanography. 1972;2(3):294-301.

[2] George AM, Kay A. Warm discharges in cold fresh water: 2. Numerical simulation of laminar line plumes. Environmental Fluid Mechanics. 2017;17:231-46.

[3] George AM, Kay A. Numerical simulations of a line plume impinging on a ceiling in cold fresh water. International Journal of Heat and Mass Transfer. 2017;108:1364-73.

[4] Macqueen JF. Turbulence and cooling water discharges from power stations. Mathematical Modelling of Turbulent Diffusion in the Environment. 1979:379-437.

[5] Marmoush YR, Smith AA, Hamblin PF. Pilot experiments on thermal bar in lock exchange flow. Journal of Energy Engineering. 1984;110(3):215-27.

[6] Hoglund B, Spigarelli SA. Studies of the sinking plume phenomenon. In: Proceedings of the 15th conference on great lakes research. International Association of Great Lakes Research, Ann Arbor. 1972;614 - 624.

[7] Bukreev VI, Gusev AV. The effect of densification during mixing on the spreading of a vertical round jet. Doklady Earth Sciences. 2011;439(1):1002-1005.

[8] Lin W, Armfield SW. Direct simulation of weak axisymmetric fountains in a homogeneous fluid. Journal of Fluid Mechanics. 2000;403:67-88.

[9] Lin W, Armfield SW. Direct simulation of weak laminar plane fountains in a homogeneous fluid. International journal of heat and mass transfer. 2000;43(17):3013-26.

[10] Lin W, Armfield SW. The Reynolds and Prandtl number dependence of weak fountains. Computational Mechanics. 2003;31(5):379-89.

[11] Srinarayana N, McBain GD, Armfield SW, Lin WX. Height and stability of laminar plane fountains in a homogeneous fluid. International Journal of Heat and Mass Transfer. 2008;51(19-20):4717-27.

[12] Srinarayana N, Armfield SW, Lin W. Behaviour of laminar plane fountains with a parabolic inlet velocity profile in a homogeneous fluid. International journal of thermal sciences. 2013;67:87-95.

[13] Srinarayana N, Williamson N, Armfield SW, Lin W. Line fountain behavior at low-Reynolds number. International journal of heat and mass transfer. 2010;53(9-10):2065-73.

[14] Williamson N, Srinarayana N, Armfield SW, McBain GD, Lin W. Low-Reynolds-number fountain behaviour. Journal of Fluid Mechanics. 2008;608:297-317.

[15] Burridge HC, Mistry A, Hunt GR. The effect of source Reynolds number on the rise height of a fountain. Physics of Fluids. 2015;27(4):047101.

[16] Caulfield CC, Woods AW. Plumes with non-monotonic mixing behaviour. Geophysical Astrophysical Fluid Dynamics. 1995;79(1-4):173-99.

[17] Morton BR, Taylor GI, Turner JS. Turbulent gravitational convection from maintained and instantaneous sources. Proceedings of the Royal Society of London. Series A. Mathematical and Physical Sciences. 1956;234(1196):1-23.

[18] Kay A. Warm discharges in cold fresh water. Part 1. Line plumes in a uniform ambient. Journal of Fluid Mechanics. 2007;574:239-71.

[19] Turner JS. Jets and plumes with negative or reversing buoyancy. Journal of Fluid Mechanics. 1966;26(4):779-92.

[20] Moore DR, Weiss NO. Nonlinear penetrative convection. Journal of Fluid Mechanics. 1973;61(3):553-81.

[21] Oosthuizen PH, Paul JT. A numerical study of the steady state freezing of water in an open rectangular cavity. International Journal of Numerical Methods for Heat Fluid Flow; 1996.

[22] COMSOL Multiphysics Cyclopedia. The Finite Element Method (FEM). [ONLINE]
Available at: https://www.comsol.com/multiphysics/finite-element-method [Accessed 28 April 2016].

[23] Vinoth BR, Panigrahi PK. Characteristics of low Reynolds number non-Boussinesq fountains from non-circular sources. Physics of Fluids. 2014;26(1):014106.

[24] Osaisai EF, George AM. A Numerical Study of the behaviour on Lock Volume Variations in Lock-Exchange Density Current in Cold Fresh Water. Journal of Scientific Research and Reports. 2022:125-41.

[25] George MA, Osaisai FE. Density Current Simulations In Cold Fresh Water And Its Cabbeling phenomenon: A Comparative Analysis With Given Experimental Results. Current Journal of Applied Science and Technology. 2022;41(29):37 - 52.

[26] Osaisai EF, George AM. Propagation Speed of the Frontal Head Through Lock-Exchange Density Current in Cold Fresh Water: Simulations without the Effect of Back-reflected Waves. Asian Research Journal of Mathematics. 2022;18(11):249-60.

[27] Lin WE, Armfield SW. Very weak fountains in a homogeneous fluid. Numerical Heat Transfer: Part A: Applications. 2000;38(4):377-96.

Peer-review history:
The peer review history for this paper can be accessed here (Please copy paste the total link in your browser address bar)
https://www.sdiarticle5.com/review-history/96739